A 250-GHz ESR Study of Highly Distorted Manganese Complexes†

W. Bryan Lynch, R. Samuel Boorse, and Jack H. Freed*

Contribution from the Baker Laboratory of Chemistry, Cornell University, Ithaca, New York 14853

Received June 25, 1993®

Abstract: ESR spectra at 250 GHz and magnetic fields ranging from 45 to 95 kG have been measured for the compounds $Mn(\gamma\text{-picoline})_4X_2$ and $Mn(o\text{-phenanthroline})_2X_2$, where X = Cl, Br, and I. These spectra are in the high-field limit and well resolved; hence, they are inherently simple to analyze. We find these spectra to be very sensitive to the precise values of the zero-field splitting (zfs) parameters. Thus D and η (E/D) can be estimated directly from the spectrum, with very accurate values obtained using third-order perturbation theory for the electron spin Hamiltonian of high-spin Mn^{2+}. The contributions of all five allowed electron spin transitions are observed and successfully simulated. The γ-picoline complexes have axial symmetry and D increases from 0.186 to 0.999 cm^{-1} with the size of the halogen. The o-phenanthroline complexes show a wide range of rhombic distortion and E increases linearly with the magnitude of D. The chloride compound is nearly axial (D = 0.124 cm^{-1}, η = 0.04), while the iodide compound is highly distorted (D = 0.590 cm^{-1}, η = 0.246). To demonstrate the applicability of the high-frequency ESR technique to biological samples, we have also measured the high-field spectrum of Mn(II) protoporphyrin IX and determined its zfs parameters to be D = 0.775 cm^{-1} and η = 0.048.

Introduction

Studies of the manganese d^5 ion in environments distorted from cubic symmetry are of importance in materials chemistry, inorganic chemistry, and biochemistry.[1-3] ESR has been used to determine the zero-field splitting (zfs) parameters (D and E), and hence the structure and stereochemistry of manganese-containing proteins and inorganic complexes as well as Mn(II) doped in crystals and powders.[1,3-8] The vast majority of work has been done using conventional X (9 GHz) and Q (35 GHz) band spectrometers. The study of ions having large zfs parameters requires the analysis of a complicated spectrum taken in the low-field limit, where D is much larger than the Zeeman energy. Theoretical analyses of such spectra have lead to the assignment of several lines in the X-band spectrum: a single line located near g_{eff} = 2.0 indicates that the system has cubic symmetry; lines near g_{eff} = 2.0 and g_{eff} = 6.0 indicate axial symmetry; a line near g_{eff} = 4.27 indicates rhombic symmetry where $E \approx {}^1/_3D$. In 1968 Dowsing and Gibson[9] calculated the ESR line positions for a d^5 system for a range of D and E values and they reported their results in the form of graphs, plotting line positions versus the D parameter for several values of η ($\eta = E/D$). Subsequent to these calculations, they reported on manganese complexes showing a variety of axial and rhombic splittings, and they successfully used their calculations to obtain values for the zfs parameters.[10-12] Since then many workers have also taken advantage of this pioneering work and have been able to interpret their spectra based upon the published graphs.

Although the study of Mn(II) at X- and Q-band has been quite successful, there is a genuine need to study these compounds in the high-field limit where the Zeeman energy is much larger than the zfs, since this leads to much more readily interpretable spectra. In addition, the line width of polycrystalline samples at X-band can be a large percentage (10%) of the total sweep width of the spectrum and small spectral features may be lost.

We have reported on a high-resolution, far-infrared ESR spectrometer in which the field for a g = 2 line is approximately 90 kG.[13] The frequency of the spectrometer is 249.9 GHz or 8.336 cm^{-1}. One of our goals is to use this instrument for the study of the zfs in metal-containing biological systems and exchange coupling in metal clusters. A necessary prerequisite is to examine compounds which, ideally, have been studied previously at low frequencies and will serve as models for metal ions in biological systems. We report here the results of our work with a series of "model" manganese complexes in the high-field limit. The complexes are MnL_4X_2 and MnC_2X_2, (L = unidentate ligand, C = bidentate ligand, and X = halide). They encompass a wide range of D and E values and show lines having g_{eff} values near 2.0, 6.0, and 4.27 at X-band. We find that the high-field spectra of these powder compounds are inherently simple, and estimates of D and E can be *measured directly* from the spectra. The line widths are about the same as at X-band. Consequently they are only 1% of the total sweep width for a D value of about 6 kG. This leads to remarkable spectral resolution compared to that at X-band. Rather than reporting graphs of line positions, we are able to obtain acceptable *fits* of our spectra using third order perturbation theory of the spin Hamiltonian. Our simulations reveal that the high-field spectrum is extremely sensitive to the values of D and E and allow for an accurate determination of

† Supported by NSF Grant No. CHE312167 and NIH Grant No. RR07126.
* Abstract published in *Advance ACS Abstracts,* October 15, 1993.

(1) Misra, S. K.; Sun, J.-S. *Magn. Reson. Rev.* **1991**, 16, 57–100.
(2) Chiswell, B.; McKenzie, E. D.; Lindoy, L. F. In *Comprehensive Coordination Chemistry*; Wilkinson, G.; Gillard, R. D.; McCleverty, J. A., Eds.; Pergamon: Oxford, 1987; Vol. 4, pp 1–122.
(3) Reed, G. H.; Markham, G. D. In *Biological Magnetic Resonance*; Berliner, L. J.; Reuben, J., Eds.; Plenum: New York, 1984; Vol. 6, pp 73–142.
(4) Luck, R.; Stosser, R.; Poluektov, O. G.; Grinberg, O. Ya.; Lebedev, Ya. S. *Z. Anorg. Allg. Chem.* **1992**, 607, 183–187.
(5) Xu, Y.; Chen, Y.; Ishizu, K.; Li, Y. *Appl. Magn. Reson.* **1990**, 1, 283–294.
(6) Shepherd, R. A.; Graham, W. R. M. *J. Chem. Phys.* **1984**, 81, 6080–6084.
(7) Woltermann, G. M.; Wasson, J. R. *Inorg. Chem.* **1973**, 12, 2366–2370.
(8) Meirovitch, E.; Poupko, R. *J. Phys. Chem.* **1978**, 82, 1920–1925.
(9) Dowsing, R. D.; Gibson, J. F. *J. Chem. Phys.* **1969**, 50, 294–303.
(10) Dowsing, R. D.; Gibson, J. F.; Goodgame, M.; Hayward, P. J. *J. Chem. Soc. (A)* **1969**, 187–193.
(11) Dowsing, R. D.; Gibson, J. F.; Goodgame, D. M. L.; Goodgame, M.; Hayward, P. J. *J. Chem. Soc. (A)* **1969**, 1242–1248.
(12) Goodgame, D. M. L.; Goodgame, M.; Hayward, P. J. *J. Chem. Soc. (A)* **1970**, 1352–1356.
(13) Lynch, W. B.; Earle, K. A.; Freed, J. H. *Rev. Sci. Instrum.* **1988**, 59, 1345–1351.

0002-7863/93/1515-10909$04.00/0

these parameters. We also present an example of a biologically relevant manganese compound, which has been studied previously[14] at X-band.

Experimental Section

Sample Preparation. Most of the manganese halide complexes studied have been prepared previously.[15-17] Our compounds were prepared in a similar manner, in most cases using ethanol as a solvent and heating the reaction mixture to between 30 and 60 °C for 10 min. The resultant precipitate was filtered and washed with ether. The powder composition for the $Mn(\gamma\text{-picoline})_4Cl_2$ compound was confirmed by IR.[16] Many of the powders were heated to about 50°C for 2–3 h under flowing nitrogen to drive off any remaining solvent, although this had little, if any, effect on the ESR spectra. The picoline compounds were white or dirty-white and the *o*-phenanthroline compounds appeared yellow. The iodide complexes were prepared and stored in the dark to prevent formation of iodine. ESR studies were made of the neat powders at the ambient temperature of our instrument, which is typically 0–5°C.

Mn protoporphyrin IX has been prepared previously.[18,19] The identity of the raw material was verified with UV–vis,[19] and the material was used without further purification. A minimum amount of pH 7.0 aqueous phosphate buffer was added to the material to form a paste. Reduction from Mn(III) to Mn(II) was accomplished by adding a small amount of sodium dithionite. ESR spectra were taken of the frozen mixture at about 120 K.

Instrumentation. The far-infrared ESR spectrometer has been described previously.[13] The semiconfocal Fabry–Perot cavity (Figure 1) is composed of two horn/mirror pieces constructed of tellurium–copper alloy and embedded in epoxy. The metal is no more than 0.25 mm thick at any one place to reduce skin-depth effects as much as is practical. The coupling holes into and out of the cavity are 1.18 mm in diameter. The modulation coil is quite small, and it gives a maximum amplitude of at least 50 G at 100 kHz. Amplitudes used in this study were usually 5 G at 100 kHz. The magnet was swept at a rate of no greater than 25 G/s. A 0.001 ohm precision resistor (American Magnetics Inc.), in series with the magnet and its power supply, and a Sentec 1101 teslameter were used to calibrate the field sweep of the magnet. The field sweep is extremely linear, and field measurements are believed to have a precision of at least ±6 G (i.e., 6 parts in 10^5). The maximum field value attainable is 95 kG at 4.2 K.

X-band spectra were taken at room temperature with a Bruker ER 200D spectrometer.

Theory

The spin Hamiltonian for Mn^{2+} ($S = {}^5/_2, I = {}^5/_2$) in a quadratic crystal field is given by

$$\mathcal{H} = g\beta\mathbf{H}\cdot\mathbf{S} - g_N\beta_N\mathbf{H}\cdot\mathbf{I} + a\mathbf{I}\cdot\mathbf{S} + \mathcal{H}_{zfs}$$

where the first three terms represent the electronic and nuclear Zeeman interactions and the electron-nuclear hyperfine interaction, respectively. H_{zfs} is the zero-field splitting term which can be written

$$\mathcal{H}_{zfs} = D\left\{S_z^2 - \frac{1}{3}S(S+1)\right\} + \frac{E}{2}\{S_+^2 + S_-^2\}$$

Here, z is the main principal axis of the zfs tensor. D and E are the axial and rhombic zfs parameters. We assume g and a are isotropic. The spin Hamiltonian can be written as

$$H = H^{(0)} + H^{(1)}$$

$$H^{(0)} = g\beta HS_z$$

where the direction of the magnetic field H (z axis) was chosen as the axis of quantization. Expressions for the perturbation energies, up to third-order, have been written down before.[8,20] They are

$$E_{Mm}^{(0)} = g\beta HM$$

$$E_{Mm}^{(1)} = aMM - g_N\beta_N Hm + a\left\{M^2 = \frac{1}{3}S(S+1)\right\}$$

$$E_{Mm}^{(2)} = \frac{a^2}{2\omega}\{MI(I+1) - mS(S+1) + M^2m - Mm^2\} + \frac{2B_+B_-}{\omega}\{8M^3 + M - 4MS(S+1)\} + \frac{2C_+C_-}{\omega}\{2M^3 + M - 2MS(S+1)\}$$

$$E_{Mm}^{(3)} = \frac{AB_+B_-}{\omega^2}\{S_M^+(2M+1)^3 - S_M^-(2M-1)^3\} + \frac{AC_+C_-}{\omega^2}\{(M+1)S_M^+S_{M+1}^+ - (M-1)S_M^-S_{M-1}^-\} + \frac{Re(B_+^2C_-)}{\omega^2}\{(2M+1)(2M+3)S_M^+S_{M+1}^+ + (2M-1)(2M+3)S_M^-S_{M-1}^- - 2(2M-1)(2M+1)S_M^-S_M^+\} + \frac{a^3}{4\omega^2}\{(-M+m-1)S_M^+I_m^- + (M-m-1)S_M^-I_m^+\} + \frac{aB_+B_-}{\omega^2}\frac{2m}{M}\{[S(S+1) - M^2]^2 - M^2\} + \frac{aC_+C_-}{2\omega^2}m\{S_M^+S_{M+1}^+ - S_M^-S_{M-1}^-\} + \frac{a^2A}{4\omega^2}\{(2M+1)S_M^+I_m^- - (2M-1)S_M^-I_m^+\}$$

where

$$A = D\left\{\left(\frac{3\cos^2\theta - 1}{2}\right) + \frac{3}{2}\eta\sin^2\theta\cos 2\phi\right\}$$

$$B_\pm = \frac{D}{4}\{-\sin 2\theta + \eta\sin 2\theta\cos 2\phi \pm i2\eta\sin\theta\sin 2\phi\}$$

$$C_\pm = \frac{D}{4}\{\sin^2\theta + \eta(\cos^2\theta + 1)\cos 2\phi \pm i2\eta\cos\theta\sin 2\phi\}$$

$$\eta = \frac{E}{D}$$

$$\omega = g\beta H$$

$$S_M^\pm = S(S+1) - M(M\pm 1)$$

$$I_m^\pm = I(I+1) - m(m\pm 1)$$

M and m are the z-components of the electronic and nuclear spin angular momentum, and θ and ϕ are the polar and azimuthal angles between the magnetic field and the coordinate system of the zfs tensor. Only the first-order term of the nuclear Zeeman energy is retained because of its small magnitude.

These expressions were used to calculate the energies of the allowed electronic spin transitions $|M,m\rangle \leftrightarrow |M-1,m\rangle$ between *all five* electronic spin states. Our calculations were done in the field swept manner by requiring the frequency of the transition to be constant at 249.9 GHz (8.336 cm^{-1}), which is the exact frequency of our spectrometer. Then, for a given set of θ and ϕ

(14) Yonetani, T.; Drott, H. R.; Leigh, Jr., J. S.; Reed, G. H.; Waterman, M. R.; Asakura, T. *J. Biol. Chem.* **1970**, 245, 2998–3003.
(15) Allen, J. R.; Brown, D. H.; Nuttall, R. H.; Sharp, D. W. A. *J. Inorg. Nucl. Chem.* **1965**, 27, 1865–1867.
(16) Goodgame, M.; Hayward, P. J. *J. Chem. Soc. (A)* **1966**, 632–634.
(17) Schaeffer, W. D.; Dorsey, W. S.: Skinner, D. A.; Christian, C. G. *J. Am. Chem. Soc.* **1957**, 79, 5870–5876.
(18) Taylor, J. F. *J. Biol. Chem.* **1940**, 135, 569–595.
(19) Yonetani, T.; Asakura, T. *J. Biol. Chem.* **1969**, 244, 4580–4588.
(20) Markham, G. D.; Rao, B. D. N.; Reed, G. H. *J. Magn. Reson.* **1979**, 33, 595–602.

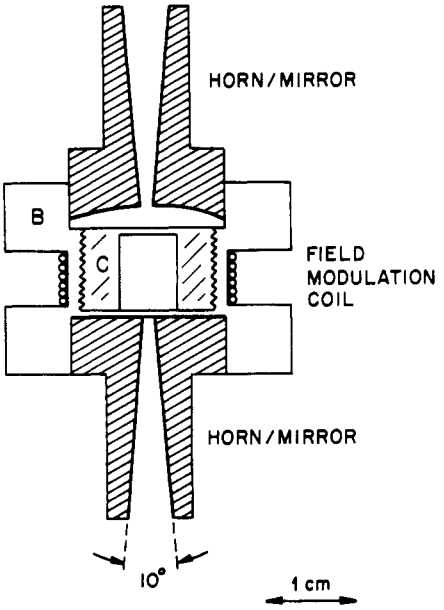

Figure 1. Fabry–Perot cavity for ESR of metal ions at 250 GHz. The body (B) of the cavity is made of Teflon and houses the field modulation coil. Above and below the body are the horn/mirror assemblies, which are made of 0.25-mm thick tellurium–copper alloy embedded in epoxy for support. The coupling holes are 1.18 mm in diameter, and the radius of curvature of the spherical mirror is 2.54 cm (1 in.). The sample is contained within the Teflon chamber (C) which screws into the body of the cavity. Windows (Teflon) above and below the sample are 0.43 mm thick. Tuning is accomplished by moving the spherical mirror relative to the flat mirror.

values, resonance field positions were calculated using a Newton–Raphson routine.[21] The transition probability of the absorption spectrum was calculated using the expression

$$\text{intensity} \propto |\langle Mm|S_+ + S_-|M'm\rangle|^2$$

Our spectra cover a wide range of magnetic field values, resulting in a variation of the Boltzmann factor. However, this variation in relative intensities over the width of our spectra is no more than 2%; hence, we have neglected any contributions due to Boltzmann effects. The derivative spectrum was calculated from the absorption using a convolution technique and assuming a Lorentzian line shape. Line broadening due to a distribution in D and E parameters was not necessary for fitting our spectra. Simulations were calculated using a Convex computer at the Cornell University Materials Science Center.

Results

Figure 2 sketches the first-order predictions of perturbation theory in the high-field regime for the canonical orientations as well as higher order predictions for the $+^1/_2 \leftrightarrow -^1/_2$ transition. For the axially symmetric case (Figure 2a) lines are spaced symmetrically about $g \approx 2$, the spacing being dependent only upon the value of D. (The letters x, y, and z represent the orientation of the field with respect to the zfs tensor axes.) Although higher order terms will break the symmetry of the spectrum, they also cause a large splitting in the $+^1/_2 \leftrightarrow -^1/_2$ transition. This transition is split into three turning points, the typical 0° (z) and 90° (x,y) transitions as well as a line at 41.8° that has been observed previously by many workers.[5,6] Because of the simplicity of the axial high-field spectrum, estimates of D can be made directly from the spectrum. The effects of rhombic distortion, E, are to cause splittings in many, but not all, of the transitions. The case of full rhombic distortion, $E = {}^1/_3D$, is

(21) Press, W. H.; Teukolsky, S. A.; Vetterling, W. T.; Flannery, B. P. *Numerical Recipes in Fortran*; Cambridge University Press: Cambridge, 1992; pp 355–360.

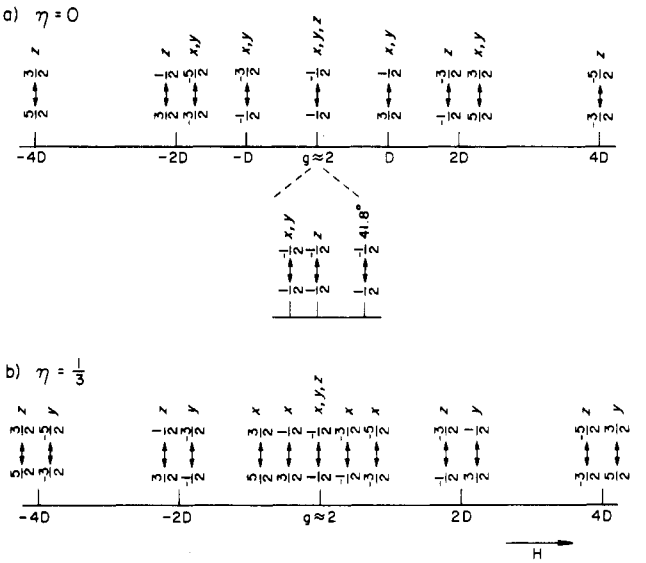

Figure 2. Schematic diagram of first-order predictions for the Mn^{2+} ESR in the high-field regime. Positions of the transitions are indicated as relative to the $g \approx 2$ field value. (a) $\eta = 0$; splittings in the $+^1/_2 \leftrightarrow -^1/_2$ transition as a result of higher-order terms are shown below. (b) $\eta = {}^1/_3$.

shown in Figure 2b. The positions of the 0° or z transitions are insensitive to E, and their positions are unchanged from the axial case. However, lines $\pm D$ from $g \approx 2$ are heavily dependent upon the amount of rhombic distortion, because they are in-plane transitions. As E is increased from zero, the degeneracy of these two lines is lost, and the y transition moves toward the outer transitions while the x transition moves toward the inner transitions. A similar splitting occurs in the x and y transitions at $\pm 2D$. At full rhombic distortion, the $\pm D$ lines are lost, and we are left with lines only at $g \approx 2$, $\pm 2D$, and $\pm 4D$. Lines near $g \approx 2$, which in the axial case were due only to the $+^1/_2 \leftrightarrow -^1/_2$ transition, now contain all the other x transitions as well. Depending upon the value of D and the line width, this region of the spectrum may appear as a single line or a complex pattern of many lines. Because of the sensitivity of the spectrum to the value of E, it is quite easy to determine the amount of rhombic distortion from a spectral simulation.

Figures 3–9 show spectra of our manganese compounds along with our best fits using third-order perturbation theory. Note that the maximum magnetic field available to us is 95 kG, so only those lines below 95 kG are observed. For the Mn protoporphyrin IX sample, lines greatly removed from $g \approx 2$ are very weak, and the spectrum shown is the average of six scans. Line widths are 500–1000 G, most likely due to spin exchange[10] in the neat samples. As a result, hyperfine splittings are not observed in our spectra. (Hyperfine splitting is observed near $g \approx 2$ in the Mn protoporphyrin IX spectrum. This signal, with a 20 G line width, is most probably due to "free manganese" or $Mn(H_2O)_6^{2+}$, in which the metal ion resides in a largely cubic environment.) Consequently, in all of our fits the hfs parameter, a, was given the value zero. Table I lists the g values, zfs parameters, and line widths for the various samples, as obtained from our best fits. There is little systematic variation in g values amongst the halides. g values can be determined to only three decimal places because of the large line widths. Errors in D and E (1 and 2%, respectively) were estimated by determining the range in values for which acceptable fits were found. The small size of our error estimate reflects the quality of the fits we are able to achieve.

Discussion

$Mn(\text{-picoline})_4X_2$ Complexes. This series of halides has been studied previously at X-band frequencies by Dowsing and co-

Table I. 250-GHz Results

ligand	halide	g value[a]	D^b (cm^{-1})	E^c (cm^{-1})	η^d	width (G)
γ-picoline	Cl	2.004	0.186	0	0	400
	Br	2.002	0.626	≤0.003	≤0.005	650
	I	2.001	0.999	≤0.005	≤0.005	600
o-phenanthroline	Cl	2.000	0.124	0.005	0.04	600
	Br	2.002	0.359	0.074	0.21	675
	I	2.008	0.590	0.145	0.246	750
protoporphyrin IX		2.001	0.775	0.037	0.048	1000

[a] Estimated error is ±0.001. [b] Estimated error is ±1%. [c] Estimated error is ±2%. [d] Estimated error is ±1 in the last digit.

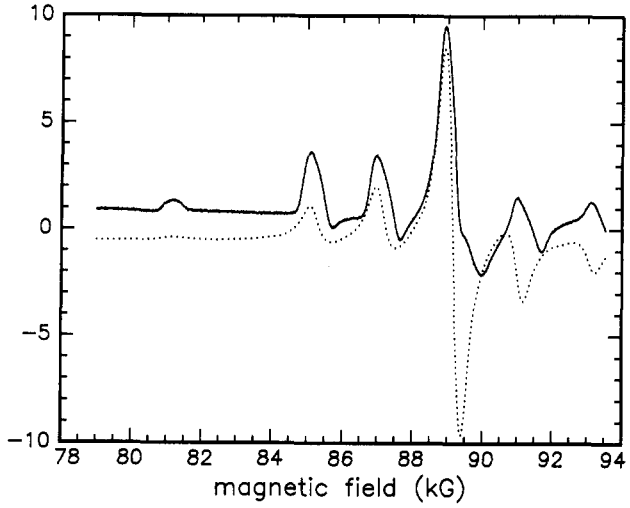

Figure 3. 250-GHz ESR of Mn(γ-picoline)$_4$Cl$_2$ (—) with simulation (···) using g = 2.004, D = 0.186 cm^{-1}, η = 0, and line width = 400 G.

workers.[10] The major features they observed are lines at g_{eff} = 6.0 and g_{eff} = 2.0, which are due to transitions within the lowest Kramers doublet for an axially symmetric system. Other lines observed were used to determine the values of D and η. Our X-band spectra (not shown) are very similar to those reported earlier, giving us confidence that we are studying the same complexes. Figures 3–5 show the high-field spectra of the chloride, bromide, and iodide complexes, respectively, along with our best fits. It is apparent from these results that third-order perturbation theory provides a satisfactory description of our high-field results. Line positions and intensities are well accounted for. It is interesting, and satisfying, that the $-4D$ line, which we predict to have relatively little intensity, actually is quite strong and is easily observed in our spectra.

Table II compares the zfs parameters determined by previous X-band work[10] and our high-field study. The bromide and iodide complexes have strong axial distortions with high values for D and very small values for η. The high-field results are similar to the X-band results with our D values about 15% higher. The agreement between experiment and simulation shown in Figures 4a and 5a is very good, especially for the iodide compound. For the bromide complex, most of the peaks are fit well, but we find we cannot adequately fit the large splitting between the 41.8° and 90° turning points of the $+^1/_2 \leftrightarrow -^1/_2$ transition (but see below). Such a large splitting would require a D value much larger than that needed to fit the rest of the spectrum at lower fields. The small lines at 47 and 58 kG in Figure 5a are believed to be due to impurities. Note the presence of a shoulder on the main line at 69 kG (the $-2D$ line) in the iodide simulation (Figure 5a). The shoulder is the $^3/_2 \leftrightarrow {}^1/_2 z$ transition, which, at such a high value of D, is not exactly degenerate with the $-^3/_2 \leftrightarrow -^5/_2 x,y$ transition. We observe this shoulder in the experimental spectrum as a slight broadening at the base of the line. Because of the sensitivity of the high-field spectrum to small changes in η, we are able to determine that η in these two compounds is in

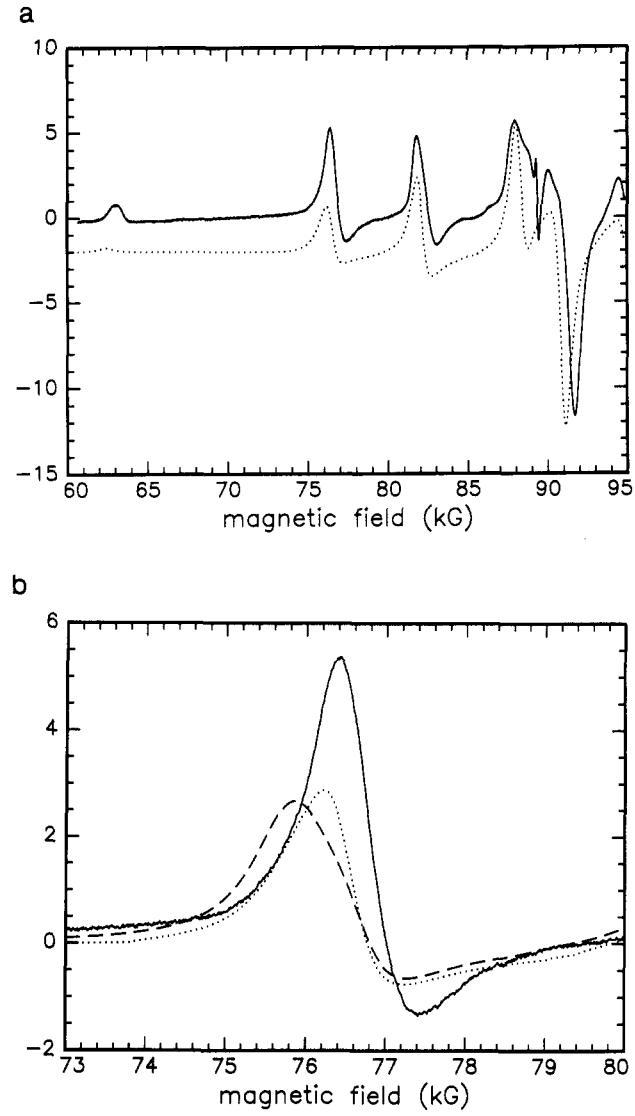

Figure 4. (a) 250-GHz ESR of Mn(γ-picoline)$_4$Br$_2$ (—) with simulation (···) using g = 2.002, D = 0.626 cm^{-1}, η = 0, and line width = 650 G. (b)250-GHz ESR of the $-2D$ line for Mn(γ-picoline)$_4$Br$_2$ (—) with simulations using η = 0 (···) and η = 0.01 (– –). Other parameters are the same as in part a.

fact smaller than the X-band value of 0.01. Figures 4b and 5b show the $-2D$ line for the bromide and iodide complexes, respectively, along with simulations of that line for η values of 0 and 0.01. The simulations with η values of 0.01 are clearly much broader than the observed spectra, and so η must be smaller than 0.01. Since there is little difference between simulations of the $-2D$ line with η = 0 and 0.005, we report our results in Tables I and II as $\eta \leq 0.005$ for these two complexes. The simulations presented in Figures 4a and 5a have an η value of 0.

Previous X-band studies[10] of the Mn(γ-picoline)$_4$Cl$_2$ complex indicate a small D value of 0.16 cm^{-1} and η = 0.10, much larger than in the bromide and iodide systems. (See Table II.) Our high-field spectrum (Figure 3) is not as complex as what we would expect for a system having the above zfs parameters. The simulation shown in Figure 3 is for an axial system (η = 0) having a D value of 0.186 cm^{-1}, which accounts well for the observed features in the high-field spectrum. It is satisfying that the calculated D value is quite similar to that determined from previous X-band work,[10] but the values for η differ greatly. If η were equal to 0.10, the transitions at 85 and 87 kG each would have split into lines moving to higher and lower magnetic fields. We do not observe such splittings. We are not certain of the origin of the skewed line shape of the $-D$ and $-2D$ lines. A small amount

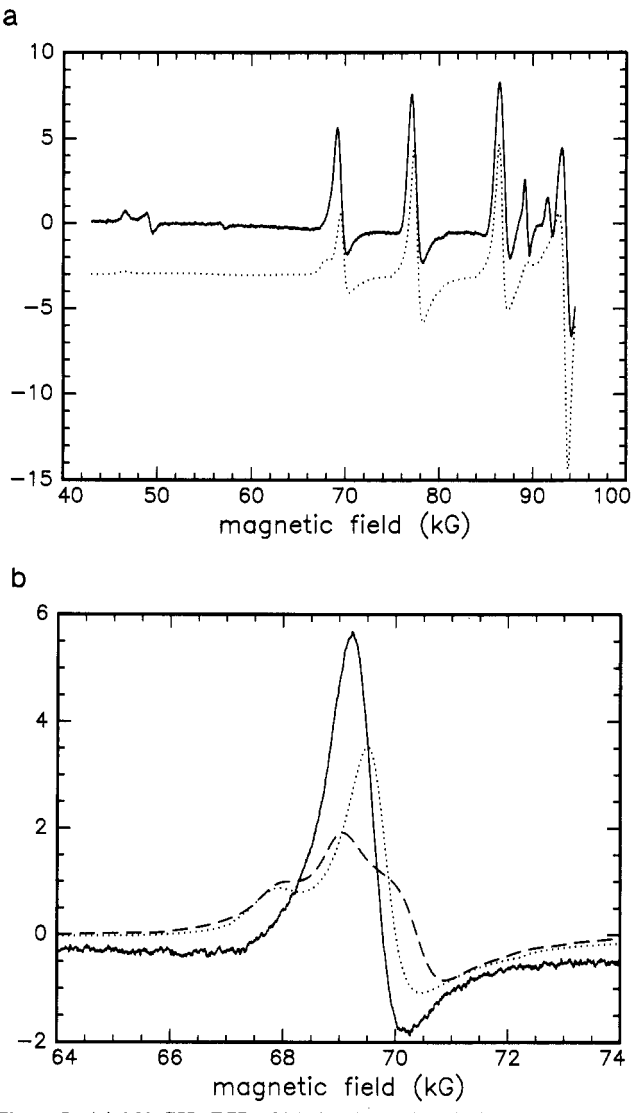

Figure 5. (a) 250-GHz ESR of Mn(γ-picoline)$_4$I$_2$ (—) with simulation (···) using g = 2.001, D = 0.999 cm^{-1}, η = 0, and line width = 600 G. (b)250-GHz ESR of the $-2D$ line for Mn(γ-picoline)$_4$I$_2$ (—) with simulations using η = 0 (···) and η = 0.01 (– –). Other parameters are the same as in (a).

Table II. Comparison of zfs Values Obtained at X-Band and at 1 mm

		D (cm^{-1})		η	
ligand	halide	X-band[a]	1 mm	X-band[a]	1 mm
γ-picoline	Cl	0.16	0.186	0.10	0
	Br	0.54	0.626	0.01	≤0.005
	I	0.87	0.999	0.01	≤0.005

[a] Reference no. 10.

of rhombic distortion ($\eta \approx 0.02$) will give a skewed shape at the $-2D$ position but not at the $-D$ position. Hence, we are unable to determine a maximum value for η, as we did with the bromide and iodide samples, and we report our value for η simply as 0. We also tried a Gaussian distribution of D, and hence η, values but this only resulted in a broadening of the lines. The disparity between experimental spectrum and simulation at fields higher than 89.5 kG indicates the presence of an impurity spectrum which overlaps and interferes with the desired spectrum. We should point out that the spectrum we obtain is strongly dependent upon the type of preparation. Figure 3 is the spectrum of a Mn(γ-picoline)$_4$Cl$_2$ sample prepared in water, according to ref 17. However, if the compound is prepared according to the method of ref 15, i.e., in refluxing γ-picoline, we obtain a complex spectrum

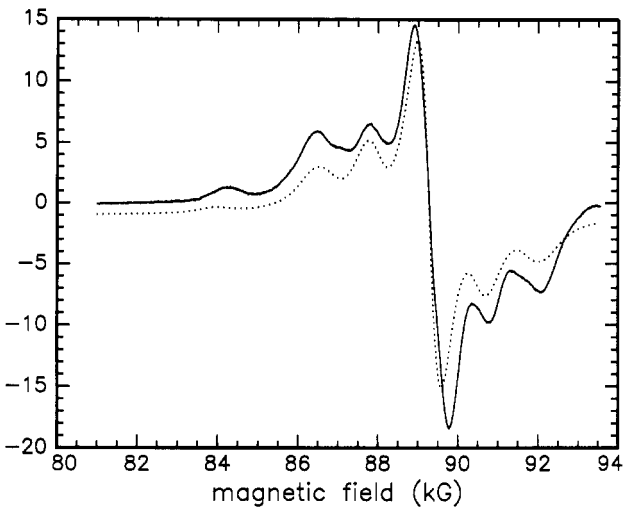

Figure 6. 250-GHz ESR of Mn(*o*-phenanthroline)$_2$Cl$_2$ (—) with simulation (···) using g = 2.000, D = 0.124 cm^{-1}, η = 0.04, and line width = 600 G.

that contains lines shown in Figure 3 but with much less intensity. The possibility exists that the 90 kG region of the Mn(γ-picoline)$_4$Br$_2$ spectrum is also distorted by an unknown impurity.

Mn(*o*-phen)$_2$X$_2$ Complexes. To our knowledge, the X-band spectrum of only the iodide complex has been presented before.[22] It shows a strong line near g_{eff} = 4.27, indicating a value of η close to $^1/_3$. However, specific values for D and η were not given. Our X-band spectrum of the iodide complex is similar to that already reported and shows a strong line at g_{eff} = 4.14. The X-band spectrum of the bromide complex shows a line at g_{eff} = 3.82, also near g_{eff} = 4.27, and we expect the zfs parameters of the iodide and bromide samples to be similar. The X-band spectrum of the chloride sample is similar to that reported for the Mn(γ-picoline)$_4$Cl$_2$ complex; hence, D and η must be small.

The high-field spectrum of Mn(*o*-phen)$_2$Cl$_2$ (Figure 6) is quite simple, and, because of a low D value (0.124 cm^{-1}), we are almost able to observe the complete spectrum within the sweep limits of our magnet. The simulation we have chosen as our best fit contains a small amount of rhombic distortion (η = 0.04). However, because of the overlap of the transitions, it is quite possible to adequately fit the spectrum with an η value of 0, although the broadening due to the small rhombic component seems to agree better with our data. In either case, agreement between data and simulation is excellent. Note that the value of D has changed from 0.186 cm^{-1} for the Mn(γ-picoline)$_4$Cl$_2$ complex to 0.124 cm^{-1} for the Mn(*o*-phen)$_2$Cl$_2$ complex, a decrease of 33%. This decrease correlates well with the increase in the strength of the o-phenanthroline ligand, compared to that of γ-picoline.

As pointed out above, X-band results indicate a large amount of rhombic distortion in the bromide and iodide complexes, and our high-field results bear this out. Figure 7 shows the high-field spectrum for the bromide complex along with a simulation corresponding to the parameters D = 0.359 cm^{-1} and η = 0.21. Note that, with the large increase in η, most of the spectral intensity is now located near $g \approx 2$, compared to the axially symmetric Mn(γ-picoline)$_4$Br$_2$ complex. There are also more lines downfield from $g \approx 2$ in this spectrum than there are in the axially symmetric spectrum of Mn(γ-picoline)$_4$Br$_2$. Rhombic distortion has caused the x and y transitions, some of which were degenerate, or nearly so, with z transitions (see Figure 2a) to move up or downfield resulting in splittings. These splittings enable us to determine the precise value of E and subsequently η. Agreement between data and fit is very satisfying. There does appear to be a group of *three* lines between 80 and 85 kG (the $-2D$ region of the spectrum), whereas our simulation only shows *two* lines. We are not sure of the identity of the third line. As with the chloride complex, the value of D has dropped significantly by replacing

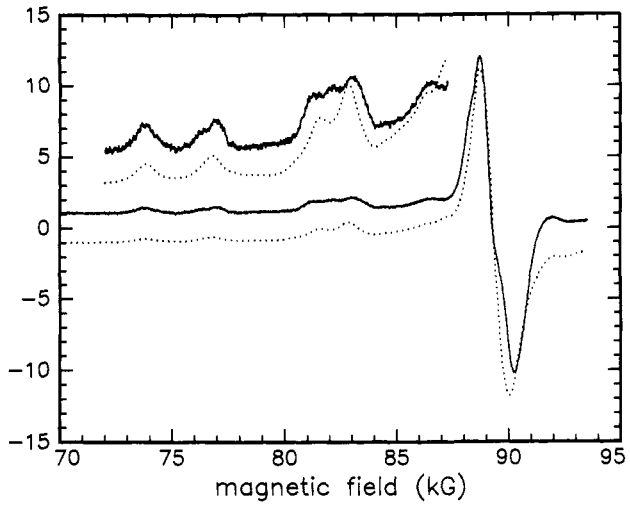

Figure 7. 250-GHz ESR of Mn(*o*-phenanthroline)$_2$Br$_2$ (—) with simulation (···) using $g = 2.002$, $D = 0.359$ cm^{-1}, $\eta = 0.21$, and line width = 675 G.

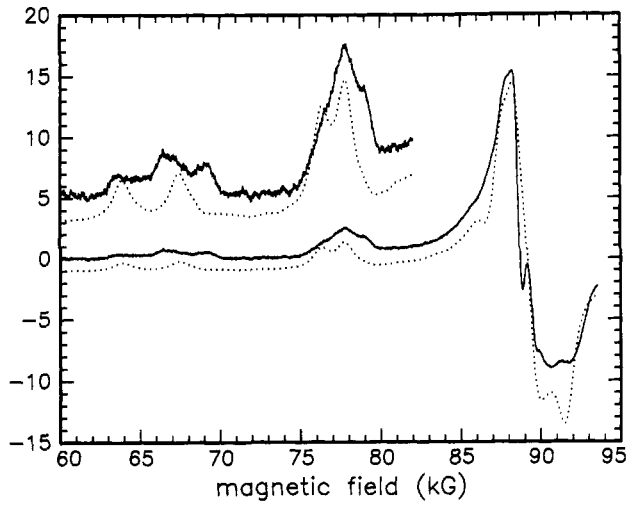

Figure 8. 250-GHz ESR of Mn(*o*-phenanthroline)$_2$I$_2$ (—) with simulation (···) using $g = 2.008$, $D = 0.590$ cm^{-1}, $\eta = 0.246$, and line width = 750 G.

the four picoline ligands with two *o*-phenanthroline ligands. The decrease in this case is 43%, which is similar to that observed in the chloride complex.

Figure 8 gives the high-field spectrum and best fit of the Mn(*o*-phen)$_2$I$_2$ complex. Like the bromide complex, most of the intensity is at $g \approx 2$, indicating a high value for D and η. Our best fit, which accounts for most of the features in this very complex spectrum, has $D = 0.590$ cm^{-1} and $\eta = 0.246$. This value of η is only somewhat higher than for the bromide complex. The presence of a small amount of impurity is seen as the small line at 89.5 kG, the intensity of which can be made to increase or decrease by adjusting the temperature at which the compound is prepared. Our sample was prepared at 30 °C in ethanol. As with the chloride and bromide complexes, the D value has again decreased by about 41% by the replacement of γ-picoline ligands with *o*-phenanthroline ligands.

As with the γ-picoline series, D also increases with the increasing size of the halogen within the *o*-phenanthroline series. However, as we have shown above, the rhombic distortion parameter, E, also increases with D. (See Table I.) The increase in E with D is linear, with a slope of 0.300, an intercept of −0.0328 cm^{-1}, and an R^2 value of 0.9999.

Mn(II) Protoporphyrin IX. Extensive studies at X and Q-band of this porphyrin and samples in which it is incorporated into a

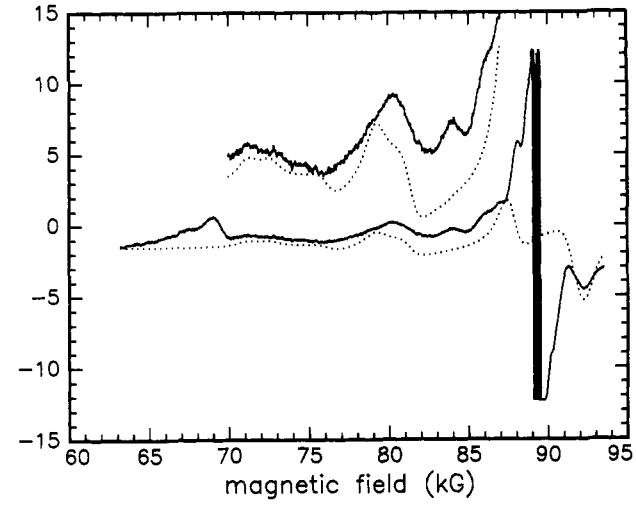

Figure 9. 250-GHz ESR of Mn(II) protoporphyrin IX (—) with simulation (···) using $g = 2.001$, $D = 0.775$ cm^{-1}, $\eta = 0.048$, and line width = 1000 G.

variety of proteins have been performed in the past.[14,23] These studies show a prominent line at $g_{eff} \approx 6.0$. Hence, η is assumed to be small, but its exact value was unknown. Values for D determined from this low-field work range from 0.5 to 0.7 cm^{-1}. The high-field spectrum of this compound is shown in Figure 9, along with our best fit. The most prominent feature of the spectrum is the sharp hyperfine lines at $g \approx 2$ due to manganese ion in a cubic environment, most probably $Mn(H_2O)_6^{2+}$. The line width of the hyperfine components is only 20G. The more important lines are much smaller in amplitude, and they enable us to determine the exact value of D. The small line at about 92 kG we believe to be the 41.8° turning point of the $+^1/_2 \leftrightarrow -^1/_2$ transition. With this assumption, and with the presence of the line at about 80 kG, which we assumed to be the $-D$ line, we are able to assign to D a value of 0.78 cm^{-1}. The fit we show is quite good, and η is fairly small, which is to be expected for this system. We have set the value of η at 0.048 so as to account for the broadening of the line at 80 kG and the small "ramp" of intensity found between 70 and 75 kG. Simulations incorporating a Gaussian distribution in D[3,8] did not give a significant improvement in fit. The $-4D$ line is not observed due to low S/N. By default, we believe the lines below 70 kG and the line at 84 kG are due to impurities.

Summary and Conclusions

We have demonstrated the application of high-field, far-infrared ESR to manganese-containing compounds having axial distortions up to 1 cm^{-1}. Because our studies were performed in the high-field regime, we are able to analyze and fit our spectra with simple third-order perturbation theory of the spin Hamiltonian and little investment in computer time. In most cases, estimates of the zfs parameters could be taken directly from the spectra. A series of "model" manganese halide complexes having a wide range of axial and rhombic distortions were successfully studied. Values for the zfs parameters were determined by fitting simulations to experiment, and these were compared to previous X-band results. In most cases agreement between X-band and high-field is good. We find close to a 40% decrease in the value of D by replacing γ-picoline ligands with *o*-phenanthroline ligands, in accord with *o*-phenanthroline being a stronger ligand than γ-picoline. This decrease is not significantly dependent upon the amount of rhombic distortion in the complexes. Both series of

(22) Dowsing, R. D.; Gibson, J. F.; Goodgame, D. M. L.; Goodgame, M.; Hayward, P. J. *Nature* **1968**, 219, 1037–1038.
(23) Hori, H.; Ikeda-Saito, M; Reed, G. H.; Yonetani, T. *J. Magn. Reson.* **1984**, 58, 177–185.

compounds show an increase in D with the size of the halogen. Within the *o*-phenanthroline series, the increase in the magnitude of E with increasing D is found to be linear. The spectrum of Mn(II) protoporphyrin IX was obtained and fit to illustrate the applicability of the technique to metal-containing biological systems.

We have also studied the high-field spectra of dilute, frozen ethanolic solutions of the same complexes above. These spectra are highly structured and give lines only 15 G wide. However, because of the lability of the manganese ion,[2] it is very difficult to know the identity of the complex(es) in solution. Indications are that more than one complex and/or isomer is present in each case. Given the complexity of such mixed spectra their further study was postponed. However, they do indicate that future studies of manganese in dilute solid solutions at high-field should yield extremely narrow lines, allowing us to observe the hyperfine splitting (hopefully in all five electronic spin transitions) for compounds with a wide range of distortions.

Acknowledgment. We thank Professor James M. Burlitch in whose laboratory the complexes were prepared and Professor Robert C. Fay and Dr. David E. Budil for helpful discussions.